Biochemistry

 Volume 42, Number 4 February 4, 2003

Current Topics

MAP Kinases and CDKs: Kinetic Basis for Catalytic Activation

John Lew*

Department of Molecular, Cell & Developmental Biology, Biomolecular Sciences & Engineering Program, University of California, Santa Barbara, California 92106

Received October 9, 2002; Revised Manuscript Received November 19, 2002

ABSTRACT: Protein kinases constitute one of the largest enzyme families encoded by the human genome. Owing to their critical role in virtually all aspects of signal transduction, protein kinases have evolved stringent mechanisms for their regulation, which classically falls into two categories: regulation by pseudosubstrate autoinhibitory domains, and remodeling of the catalytic core in response to phosphorylation and/or protein/protein interactions. While the action of pseudosubstrate domains can be explained by simple competitive autoinhibition kinetics, it is less well understood how active site phosphorylation and/or protein/protein interactions alter rates of catalysis. Here, the kinetic basis for kinase activation is discussed in relation to the MAP kinase, ERK2, and the cyclin-dependent kinase, CDK2/cyclin A, two enzymes of central importance to mammalian cell growth and division, and which serve as prototypic models of nonautoinhibitory regulation.

The history of protein phosphorylation and its role in cellular regulation is rooted in the early work on glycogen metabolism, landmarked by the discovery of glycogen phosphorylase kinase and, subsequently, cAMP[1]-dependent protein kinase (*1*, *2*). An integral part of this history was the recognition that activation of phosphorylase kinase involved direct phosphorylation by PKA, whose enzymatic activity was in turn found to be regulated by association with an inhibitory protein subunit released upon binding cAMP. This first identification of a "protein phosphorylation cascade" paved the way to the modern field of signal transduction, in which it has now been established that protein kinases universally play an important role in all aspects of cell regulation (*3*). For example, the human genome encodes 500−600 distinct protein kinase catalytic subunits, and modification by reversible phosphorylation and/or protein−protein interaction is a common theme in the regulation of virtually all members of the protein kinase superfamily.

Phylogenetic analysis has allowed the protein kinase family to be divided into several subfamilies that correlate with general themes of regulation (*4*, *5*). Mechanistically, the regulation of protein kinases can be divided into two broad classifications. The best appreciated is regulation by autoinhibition, in which inhibition of catalytic activity is achieved by interaction of the active site with a pseudosubstrate domain located within an N- or C-terminal polypeptide extension of the catalytic core (*6*). The variety of regulatory themes in protein kinases stems largely from the diversity of mechanisms employed for displacing the autoinhibitory domain from the active site resulting in kinase activation. Classic examples include the binding of Ca^{2+}/calmodulin to the autoinhibitory domains of both myosin light chain kinase and calmodulin-dependent kinase II, the

* To whom correspondence should be addressed. Tel: 805 893-5336; Fax 805 893-4724; email lew@lifesci.ucsb.edu.

[1] Abreviations: PKA, cyclic AMP dependent protein kinase; cAMP, cyclic adenosine 5′-mono-phosphate; MAPK, mitogen-activated protein kinase; ERK2, extracellular-regulated kinase 2; MBP, myelin basic protein; MEK, MAPK/ERK kinase; SAPK, stress-activated protein kinase; CDK, cyclin-dependent kinase; Csk, c-terminal src kinase; [PP], dual phosphorylated; [P], phosphorylated; [unP], unphosphorylated.

10.1021/bi0269761 CCC: $25.00
Published on Web 01/04/2003

binding of Ca^{2+} to the autoinhibitory domain of PKC, and phosphorylation of the C-terminal tail of the SRC tyrosine kinase. Also included is the binding of cAMP to the regulatory subunit of PKA in which the autoinhibitory domain of this enzyme resides on a separate polypeptide subunit [see ref *6* for review]. In all cases, autoregulation is achieved by a simple inhibition mechanism that can be considered classically competitive with respect to the binding of protein substrates at the active site.

Distinct from autoinhibitory mechanisms, phosphorylation within the kinase catalytic core has been shown to be essential for the activity of most protein kinases (*7*). On the basis of sequence homology and crystallographic information, it is clear that in all kinases activated by phosphorylation, the target site is a conserved threonine or tyrosine residue located within a defined active site segment, termed the *activation loop*. The principal roles of phosphorylation are to correctly configure the activation loop, nucleate a network of key interactions within the core, and neutralize a region of high positive charge within the active site (*8*). Thus, remodeling of the active site leading to optimized substrate binding and chemical transfer constitutes a second class of kinase regulation. While diverse mechanisms have evolved to control autoinhibition, effectively only two have been observed to affect active site configuration: phosphorylation (*7*), being general to most protein kinases, and cyclin binding, in the specific case of the cyclin-dependent kinases (*9*). The kinetic consequence of these modifications leading to activation of the protein kinase catalytic core is the focus of this review.

A principal objective of kinetic studies is to provide an essential link between atomic resolution structure and biochemical function. The first insight into the structural basis for protein kinase activity came from the X-ray crystallographic structure of PKA (*10*, *11*), which continues to serve as the prototype member of more than 30 distinct protein kinases whose structures have now been solved. Collectively, these structures reveal that all protein kinases display a globular fold consisting of an N- terminal lobe (~85 aa) that is mainly β-sheet in structure, and a larger C-terminal lobe (~170 aa) that is mostly α-helix. The interface between the two lobes constitutes the active site cleft, in which the adenine ring of ATP is deeply buried, while the γ-phosphate moiety points toward the mouth of the active site where protein substrates bind (*12*). Among approximately 10 individual amino acid residues that are highly conserved in all protein kinases, not surprisingly most are found to cluster near the active site (*13*) and are critical for catalysis (*14*). In particular, a lysine/glutamate pair (Lys^{72}/Glu^{91} in PKA) is critical for stabilizing the α- and β-phosphates of ATP for phosphoryl transfer (*15*, *16*). An aspartate residue (Asp^{166} in PKA) in the catalytic loop serves to orient the attacking substrate hydroxyl group, while another (Asp^{184} in PKA) located in a Mg^{2+} positioning loop coordinates to an essential Mg^{2+} ion. The architecture (*8*, *12*, *13*) and catalytic mechanisms (*17*) of protein kinases have been thoroughly reviewed.

In light of the abundant information accrued on protein kinase structure and, to a lesser extent, mechanism, a key question is: How is activation of the catalytic core controlled by phosphorylation and/or protein−protein interaction? While a handful of protein kinases have now been studied bearing this question in mind, two enzymes, the MAP kinase ERK2 and cyclin-dependent kinase CDK2, have drawn particular interest for a number of reasons. First, the catalytic cores of both enzymes are perhaps the most extensively regulated among all protein kinases. For example, in addition to phosphorylation at the classically conserved activation loop threonine, activation of all MAP kinases requires a second phosphorylation at a neighboring tyrosine residue (*18*), while the cyclin-dependent kinases require association with cyclin (*9*). Second, while the majority of kinases undergo phosphorylation by an autocatalytic mechanism, the MAP kinases (*18*) and CDKs (*9*) undergo phosphorylation and activation by a heterologous kinase. Phosphorylation/dephosphorylation thus truly acts as a switch that serves to regulate enzymatic activity in vivo. Experimentally, the inability to undergo phosphorylation autocatalytically conveniently allows the unphosphorylated forms of ERK2 and CDK2 to be easily generated for biophysical studies. Third, several crystal structures of both enzymes are available, including structures representing active (*19*, *20*) as well as inactive (*21*, *22*) conformers. In the case of CDK2, crystal structures in partially activated states are also available (*23*, *24*). Finally, the critical role that both ERK2 and CDK2 play in cell growth and division have generated enormous interest in their cell biology, structure, function, and regulation, and insight into their kinetic mechanism is now of interest, in part owing to their potential as targets for cancer therapeutic intervention (*25*, *26*).

MAP Kinases and CDKs. The MAP kinases and CDKs are central enzymes that regulate cell proliferation in response to mitogen signaling. The MAP kinases are traditionally divided into three subfamilies based on their sequence homology: the p38 family, the stress-activated protein kinase (SAPK) family, and the extracellular signal-regulated kinases or ERKs. While the p38 kinases and SAP kinases mediate the principal pathways activated in response to environmental stress (heat shock, osmotic shock, UV irradiation, growth factor deprivation, agents that interfere with DNA and protein synthesis) and inflammatory cytokines, the ERKs, by comparison, mediate all signaling pathways initiated by polypeptide mitogens. The best characterized to-date is the *ras*−*raf* signal transduction pathway mediated by ERK2, which serves as the prototypic member of the MAP kinase family [see refs *18* and *27* for review].

Activation of the *ras*−*raf* pathway involves extracellular growth factor stimulation of a receptor tyrosine kinase, which triggers a chain of molecular events resulting in the activation of the ras proto-oncogene via membrane recruitment of the ras guanine-nucleotide exchange factor, SOS (*28*). A hallmark of all MAP kinase signaling systems is a three tier protein kinase cascade, each member of the cascade which phosphorylates and activates the respective downstream kinase, in succession. In the *ras*−*raf* pathway, this corresponds to the Raf-1/MEK1/ERK2 module, whose activation is initiated by the binding of activated ras to Raf-1 (*18*, *27*). A principal effect of ERK2 activation is the direct phosphorylation of transcription factors leading to increased expression of the D-type cyclins, activation of CDK4/cyclin D, phosphorylation of the retinoblastoma protein, and commitment of cells to DNA replication and cell cycle progression (*28*). Control of the cell cycle itself is mediated by the cyclin-dependent kinases, for which at least nine CDK subunits and

Scheme 1

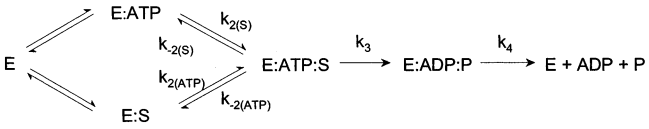

over 12 cyclins have been described. The critical CDK/cyclin complexes for core cell cycle function are CDK2/cyclin E, which drives cells across the G1/S-phase border; CDK2/cyclin A, which mediates DNA replication; and CDK1/cyclin B, which controls entry into mitosis. In all cases, CDK activity is stringently controlled by cyclin binding, phosphorylation, and the binding of protein inhibitors (*9*).

General Considerations for Kinetic Studies. In this review, we summarize the kinetic mechanisms for activation of ERK2 and CDK2 with the goal of assigning functional relevance to the structural changes observed to accompany kinase activation. Scheme 1 shows the minimal kinetic scheme for the steady-state phosphorylation of substrates catalyzed by a protein kinase under saturating concentrations of a fixed substrate. In ERK2, the mechanism has been shown to involve the random addition of substrates (*29*, *30*), which is also the inferred mechanism for CDK2 [see ref *31*]. The reactions of specific interest in Scheme 1 are the association (k_2) and dissociation (k_{-2}) of both ATP and substrates (S), phosphoryl transfer (k_3), and product release (k_4). The single arrow depicting the phosphoryl transfer step formally describes the net reaction[2] for phosphotransfer that may, or may not, in fact be thermodynamically irreversible. One approach to dissecting the detailed mechanism of catalytic activation of ERK2 and CDK2 has been to purify all enzyme species on the pathway to activation and ask how each step in the respective kinetic reaction pathway was altered in response to phosphorylation or cyclin binding. In this way, changes in the rates of substrate binding, substrate release, or phosphoryl transfer could theoretically be correlated with changes in structure.

Traditional steady-state analyses provide values for k_{cat} as well as K_m for a given enzymatic process. Both parameters are composites of multiple catalytic reaction steps, and thus do not provide direct information on any individual step specifically. For example, k_{cat} reports the net rate for substrate turnover, which comprises both the phosphoryl transfer and product release steps.[3] Furthermore, K_m is a function of all steps along the entire reaction pathway.[4] If the rate of phosphoryl transfer (k_3) is slow compared to that for the release of product (k_4), k_{cat} reflects the rate of phosphoryl transfer. If, in addition, the rate of phosphoryl transfer is slow in relation to that of substrate release (k_{-2}), K_m approximates the substrate binding affinity ($K_m \approx k_{-2}/k_2$). In general, for protein kinases whose substrates display high catalytic efficiency, it has been found that these assumptions cannot safely be made. The inability to isolate individual reaction steps along the overall reaction pathway is the prevailing limitation of enzyme structure/mechanism studies in which only steady-state kinetic parameters are obtained.

A number of methods have traditionally been employed to isolate individual kinetic steps of a reaction pathway. The most direct involve analysis in the transient-state using stopped-flow or rapid chemical quenched flow methods. Alternatively, a simple yet powerful approach has been the application of solvent viscosometric techniques in the steady-state, which involve perturbation of the relative solvent viscosity by addition of a suitable microviscosogen (*32*, *33*). Under these conditions, reactions along the catalytic pathway that involve diffusion (k_2, k_{-2}, k_4) can be separated from those that do not (k_3). At the same time, varying the substrate concentration allows substrate binding (k_2, k_{-2}) to be separated from product release (k_4). Finally, substrate association (k_2) can be separated from substrate dissociation (k_{-2}) because the rate of association is dependent upon the substrate concentration, while the rate of dissociation is not. Thus, in theory, varying both the substrate concentration as well as the relative solvent viscosity allows all steps in Scheme 1 to be isolated. Application of solvent viscosometric techniques to study protein kinase mechanism was first carried out by Adams (*34*), and has since been employed by several laboratories to investigate other members of the kinase family.

ERK2. The MAP kinases and CDKs share in common the fact that neither has evolved autoinhibition as a regulatory mechanism. Members of both enzyme families display essentially only a catalytic core domain (*13*) whose catalytic properties are controlled by remodeling of the active site in response to activation loop phosphorylation and/or cyclin binding. Members of both families require dual modification for complete activation. In the case of MAP kinases, this involves phosphorylation on a tyrosine residue conserved in all MAP kinase family members, in addition to the classically conserved threonine residue located in the activation loop. These sites conform to the consensus sequence TXY, where X, in general, corresponds to glutamic acid in the ERKs, proline in the SAPKs, and glycine in the p38 kinases. In ERK2, the sites of phosphorylation are Tyr^{185} and Thr^{183}, which are phosphorylated by a single enzyme, MEK (*18*). Although the crystal structure of ERK2 reveals the side chain of Tyr^{185} to be completely buried (*21*), phosphorylation of this site by MEK precedes that of Thr^{183} (*35*−*37*). Furthermore, dual phosphorylation by MEK appears to occur in a distributive as opposed to processive fashion, involving release of MEK after tyrosine phosphorylation followed by rebinding prior to subsequent phosphorylation at threonine (*37*, *38*).

The substrate sequence specificity of ERK2 and CDK2 has been investigated by systematic amino acid substitution analysis using model substrate peptides (*39*, *40*), as well as by selection of optimal substrate sequences by random combinatorial peptide library screening (*41*). Both MAP kinases and CDKs display an absolute requirement for proline in the substrate P_{+1} position, hence the common reference to these enzymes as proline-directed kinases. While the optimal sequence for substrate recognition by ERK2 is XPXS/TP, peptides that contain this motif are, in themselves, poor substrates (*29*), owing to the lack of additional necessary docking motifs identified in protein targets (*42*).

X-ray crystallographic structures have been solved for both unphosphorylated (*21*) and dual phosphorylated ERK2 (*19*). The major consequences of dual phosphorylation are a lateral

[2] $k_3 = \underline{k_3} * k_4/(\underline{k_{-3}} + k_4)$; where $\underline{k_3}$ and $\underline{k_{-3}}$ in this equation are the true microscopic constants for the forward and reverse reactions, respectively; k_4 is the net rate constant for release of both products.

[3] $k_{cat} = k_3 * k_4/(k_3 + k_4)$.

[4] $K_m = (k_{-2} + k_3)/k_2 * k_4/(k_3+k_4)$.

Table 1: Kinetic Constants for ERK2 and CDK2/Cyclin A

[PP]ERK2[a]		[T[160]-P]CDK2/cyclinA[b]	
K_d^{ATP} (μM)	57	K_d^{ATP} (μM)	150
K_d^{MBP} (μM)	≤0.5	K_d^{pept} (μM)	25
k_2^{MBP} (μM^{-1} s^{-1})	2.4	k_2^{ATP} (μM^{-1} s^{-1})	0.2
k_{-2}^{MBP} (s^{-1})	≤1.2	k_{-2}^{ATP} (s^{-1})	30
k_3 (s^{-1})	12	k_3 (s^{-1})	35
k_4 (s^{-1})	56	k_4 (s^{-1})	9
k_{cat} (s^{-1})	10	k_{cat} (s^{-1})	7
K_m^{ATP} (μM)	47	K_m^{ATP} (μM)	55
K_m^{MBP} (μM)	4.2	K_m^{pept} (μM)	8

[a] From Prowse et al. (*29*), substrate is MBP. [b] From Stevenson et al. (*31*), substrate is PKTPKKAKKL; also see Hagopian et al. (*47*).

rotation (5 Å) of the N- and C-terminal lobes relative to each other, and a major reorganization of the activation loop and P_{+1} substrate-binding pocket. A protein substrate, myelin basic protein (MBP), that displays high catalytic efficiency for [PP]ERK2 ($k_{cat}/K_m = 2.4 \times 10^6$ M^{-1} s^{-1}) has been used to investigate the kinetic mechanism of ERK2 (*29*). MBP binds to the active site with $K_m \approx 5$ μM and $K_d \leq 0.5$ μM, and is turned over at a maximum rate of about 10 s^{-1}. The rate of productive MBP binding occurs at the diffusion-controlled limit, meaning that every encounter with the active site results in turnover, suggestive of maximum catalytic efficiency. The rate of turnover itself is limited mostly by the rate of the phosphoryl transfer reaction, which is about 5-fold slower compared to that of product release (Table 1). The rate of phosphoryl transfer of [PP]ERK2 (12 s^{-1}) can be compared to that of CDK2/cyclin A (35 s^{-1}) (*31*), PKA (500 s^{-1}) (*43*), the tyrosine kinase, Csk (≥140 s^{-1}) (*44*), and CheA/CheY histidine kinase (650 s^{-1}) (*45*).

The large catalytic rate enhancement of ERK2 in response to dual phosphorylation has previously been quantified (*46*), but only recently has the activation mechanism been examined in kinetic detail (*52*). Dual phosphorylation causes greater than 100-fold tighter binding (K_d) of substrate MBP (*52*), an effect that is also seen in CDK2/cyclin A toward a synthetic peptide substrate (*47*). However, this is not true for either PKA or the v-fps tyrosine kinase, which display increased catalytic activities yet similar affinities for their substrates when compared to mutants whose sites of phosphorylation are substituted with nonphosphorylatable residues (*17*). Crystal structures of protein kinase/substrate complexes exist only in the case of PKA (*11*, *48*, *49*), CDK2/cyclin A (*50*), and phosphorylase kinase (*51*). Thus, the structural role of phosphorylation to enhance substrate binding affinity cannot rigorously be inferred in ERK2. However, superposition of a peptide substrate in the structure of cdk2/cyclinA (*50*) onto the active site of ERK2 shows significant steric interference between the substrate P_{+1} proline and the carbonyl oxygen of Val^{187} in [unP]ERK2 (*21*), but not [PP]ERK2 (*19*). One may speculate that this may significantly contribute to the observed ≥100-fold change in substrate binding affinity.

Activation of ERK2 also involves moderate changes (12-fold) in binding affinity for ATP (*52*). However, again it is difficult to make correlations with changes in structure for a number of reasons. First, the crystal structure of [PP]ERK2 (*19*) does not contain ATP, and second, kinetic data are available for the binding of ATP only to the ERK2·MBP complex, for which there is no structural information. Finally, the accuracies of the existing structures likely do not allow discrete changes in structure to be correlated with such moderate changes in binding energy.

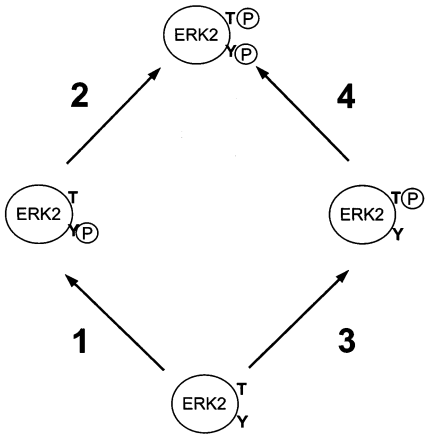

FIGURE 1: Pathways for activation of ERK2. Fold changes in kinetic parameter values corresponding to each step are given in Table 2.

Table 2: Fold Change in Kinetic Parameters for Activation of ERK2[a]

	activation step[b]			
	1	2	3	4
k_{cat}	↑1000	↑50	↑80	↑625
k_3	↑1000	↑60	↑80	↑750
K_m^{MBP}	↑1.2	↓14	↓2.5	↓4.8
K_d^{MBP}	↑1.2	↓≥120	↓2.5	↓≥40
K_m^{ATP}	↓16	↑1.1	↓1.2	↓13
K_d^{ATP}	↓23	↑1.8	↓1.2	↓11
k_{cat}^{ATPase}	↑2961	↓1.5	↑3	↑625
k_3^{ATPase}	↑2961	↓1.5	↑3	↑625
K_m^{ATPase}	↓13	↑1.5	↓1.6	↓5.5
K_d^{ATPase}	↓13	↑1.5	↓1.6	↓5.5

[a] From Prowse et al. (52). [b] See Figure 1.

While substantial effects on substrate binding are noted, the greatest effect of dual phosphorylation on catalysis is on the energetics of phosphoryl transfer, whose rate is enhanced 60 000-fold (*52*). Since this step (k_3) limits turnover in both [unP]ERK2 (by 100%) and [PP]ERK2 (by 82%), effects on the rate of phosphotransfer directly affect k_{cat}, which is enhanced 50 000-fold in response to dual phosphorylation (*52*). In accordance with classical transition state theory, such rate enhancement corresponds to differential stabilization of the transition state structure for the phosphoryl transfer reaction over that of the Michaelis ground-state complex by 6.5 kcal/mol. This can arise by stabilization of either the ATP or MBP moieties, or both. Of interest was to dissect the role of tyrosine versus threonine phosphorylation in stabilizing either or both structures in the transition-state.

Information on the role of tyrosine versus threonine monophosphorylation in the activation process, at present, comes only from kinetic studies (*53*, *54*). Crystal structures of the monophoshorylated forms of ERK2 have not yet been solved. Kinetic analysis reveals that a major role of tyrosine phosphorylation is to configure the active site for binding ATP. For example, the K_m and K_d values for ATP in both the kinase and ATPase reactions are significantly decreased upon tyrosine but not threonine phosphorylation (cf steps 1

and 3, Figure 1, Table 2) (*53*). The rate of phosphoryl transfer in the kinase reaction (k_3) is also greatly (1000-fold) enhanced, and similarly it is the ATP moiety, as opposed to that of MBP, that appears to be specifically stabilized in the transition state for phosphotransfer (Table 2). This is inferred from examination of the phosphoryl transfer reaction in the absence of MBP (k_3^{ATPase}), which shows a similar rate enhancement (2961-fold) to that found for the kinase reaction (1000-fold) in response to tyrosine, but not threonine, phosphorylation (cf steps 1 and 3, Figure 1, Table 2) (*53*). The moderate increase (80-fold) in phosphotransfer rate (k_3) in response to Thr^{183} phosphorylation (Table 2) is therefore inferred to be likely the result of optimized alignment of *MBP*, to accept the γ-phosphate.

The specific effects of Tyr^{185} phosphorylation on ATP binding and reactivity are apparent regardless of whether or not Thr^{183} is previously phosphorylated (cf steps 1 and 4, Figure 1, Table 2) (*53*). An important point is that phosphorylation at Thr^{183} plays essentially no role with respect to enhancing ATP binding or its reactivity in the activation process. Thus, optimization of the ATP binding pocket is under the complete control of phosphorylation at Tyr^{185} alone.

While optimized binding and reactivity of ATP requires only phosphorylation at Tyr^{185}, the binding of MBP depends on synergistic action between both sites. This is seen in the behavior of the K_d^{MBP} value, which is significantly lowered only after phosphorylation at *both*, as opposed to one or the other, site(s) (steps 2 and 4, Figure 1) (*53*). The contribution of tyrosine phosphorylation to MBP binding affinity is likely attributed to remodeling of the P_{+1} substrate binding pocket via hydrogen bonding between the phosphotyrosyl oxygens and the ϵ-amines of Lys^{189} and Lys^{192} in the P_{+1} pocket (*19*). On the basis of analogy with CDK2, one may speculate that displacement of the carbonyl oxygen of Val^{187} from the P_{+1} binding pocket occurs in response to phosphorylation of Thr^{183}. A definitive interpretation, however, awaits structural information on the monophosphorylated forms of ERK2.

In summary, the kinetic data put forth a relatively simple view of the activation process for ERK2 (Figure 3). ATP binding is enhanced moderately (12-fold), albeit completely, by phosphorylation at Tyr^{185}. Tyrosine phosphorylation also contributes to the overall increased affinity for MBP ($\geq$100-fold), but which is realized only upon subsequent phosphorylation at Thr^{183}. In the phosphoryl transfer reaction, ATP in the transition state is stabilized completely (1000-fold) by tyrosine phosphorylation, while MBP is stabilized (50-fold) by phosphorylation on threonine, constituting a net increase of 50 000-fold in phosphoryl transfer rate. It should be noted that interpretation of the ground-state effects are based on direct measurement, while the effects on ATP and MBP in the phosphoryl transfer reaction are by inference from studies on the ATPase reaction.

The results of Prowse et al. (*53*) should be compared with those of Zhou et al. (*54*), who have carried out independent studies on the kinetic mechanism of ERK2 activation. In the latter study (*54*), steady-state kinetic parameters were obtained on the kinase reaction using MBP and Elk-1 as substrates, as well as on the ATPase pathway. There is some discrepancy between the findings from these two groups. Zhou et al. report an increase in k_{cat} of only 9000-fold as opposed to the 50 000-fold reported by Prowse et al. in response to dual phosphorylation, and an increase of 70-fold as opposed to 2000-fold in k_{cat}^{ATPase}. These workers also observed only 2-fold reduction in K_m^{MBP} as opposed to 12-fold by Prowse et al., and 4-fold reduction in K_m^{ATP} in the ATPase reaction versus 9-fold. In particular, Zhou et al. found that phosphorylation at Tyr^{185} did not display as great an effect on enhancing k_{cat} for either MBP phosphorylation or for the ATPase reaction compared to that reported by Prowse et al. Rather, phosphorylation at each site showed more equal effects on enhancing k_{cat} for both reactions.

Prowse et al. employed mutants of ERK2 (T^{183}A, Y^{185}F) that could be phosphorylated at only one site or the other to generate the monophosphorylated species of ERK2, and these mutants displayed catalytic properties identical to the wild-type enzyme (*53*). Since the apparent differences from the two groups are seen even in studies on the wild type enzymes, it is unlikely that the mutations are the source of the experimental error. Zhou et al. generated the monophosphorylated species by dephosphorylation of [PP]ERK2 using phospho-tyrosine or phospho-serine/threonine-specific protein phosphatases (*54*). While contamination with trace amounts of [PP]ERK2, either remaining from the phosphatase treatment or generated by autophosphorylation, is the main caveat of this method, these workers were cautious that their preparations were in fact not contaminated with [PP]ERK2. Considering the rigor of both studies, it remains unclear as to the source of experimental inconsistency.

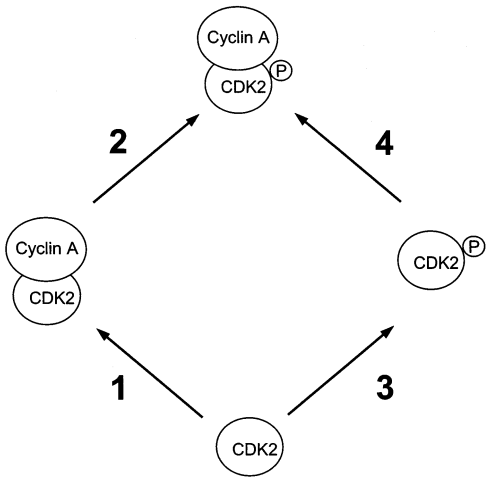

FIGURE 2: Pathways for activation of CDK2. Fold changes in kinetic parameter values corresponding to each step are given in Table 3.

Table 3: Fold Change in Kinetic Parameters for Activation of CDK2[a]

	activation step[b]			
	1	2	3	4
k_{cat}		↑270		↑8.8
k_3		↑1000		↑≤32
K_m^{H1}		↓≥144		↓≥1625
K_d^{H1}		↓≥35		↓≥480
K_m^{ATP}		↓4.2		↓37
K_d^{ATP}		↓1.4		nd[c]
k_{cat}^{ATPase}	↑25	↑1.2	↑32	↑1.1
k_3^{ATPase}	↑25	↑1.2	↑32	↑1.1

[a] From Stevenson et al. (31). [b] See Figure 2. [c] nd − could not be determined.

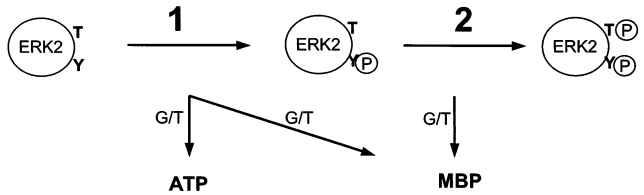

FIGURE 3: Mechanism of activation of ERK2 by tyrosine followed by threonine phosphorylation. Phosphorylation at Tyr^{185} results in maximal stabilization of ATP binding, and stabilization of MBP binding that is synergistic with phosphorylation at Thr^{183}. Subsequent phosphorylation at Thr^{183} affects only MBP. In all cases, binding of ATP and MBP is significantly enhanced in both ground (G) and transition (T) states for phosphoryl transfer.

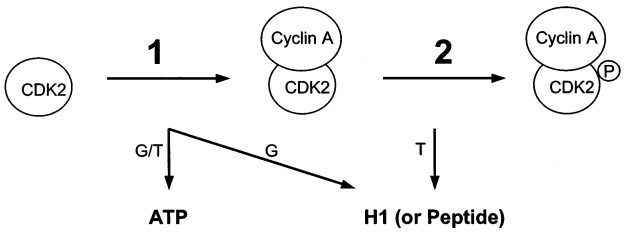

FIGURE 4: Mechanism of activation of CDK2 by cyclin binding followed by phosphorylation. Binding of cyclin A results in maximal stabilization of both the ground (G) and transition (T) state structures of ATP, and stabilizes histone predominantly in the ground state. Phosphorylation at Thr^{160} affects histone exclusively, predominantly in the transition state for phosphoryl transfer.

Importantly, Zhou et al. have characterized the kinase activity of ERK2 toward a physiological substrate, Elk-1. Elk-1 displays approximately 3-fold higher catalytic efficiency than does MBP, but the fold activation by dual phosphorylation (k_{cat}) is 6-fold less (*54*). Thus, significant differences in activation mechanism may be anticipated depending on the substrate used.

CDK2/Cyclin A. Activation of the cyclin-dependent kinases involves the binding of cyclin followed by phosphorylation within the activation loop, catalyzed by a CDK-activating kinase, CAK (*9*, *55*). The most extensive structural analysis has been carried out on CDK2, which serves as the prototypic member of the family, and for which more than 20 crystallographic structures have been solved either free or bound to cyclin A. These include [unP]CDK2 (*22*), [unP]-CDK2/cyclin A (*23*), [T^{160}-P]CDK2 (*24*), and [T^{160}-P]CDK2/cyclin A (*20*), as well as that of [T^{160}-P]CDK2/cyclin A cocrystalized with a peptide substrate (*50*), providing an unprecedented view into the structural consequences of cyclin binding and phosphorylation with respect to kinase activation.

By comparison, functional data addressing the kinetic basis for CDK activation has been sparse, and kinetic data on CDK2 are not nearly as complete as they are for ERK2. This owes largely to the complete lack of kinase activity associated with the [unP]CDK2 monomer (*24*, *31*, *56*) as well as the poor substrate binding properties of the partially activated species (*31*). The best-characterized step in the CDK2 activation process is phosphorylation of Thr^{160} in CDK2 bound to cyclin A (step 2, Figure 2). These data were collected using both histone H1 protein (*31*) as well as a short synthetic peptide as model substrates (*47*). The sequence of this peptide (PKTPKKAKKL) was originally derived from sites within histone that historically were shown to be phosphorylated by maturation promoting factor (*57*, *58*). This peptide displays the highest catalytic efficiency ($k_{cat}/K_m = 10^6\ M^{-1}\ s^{-1}$ (*47*)) toward [P]CDK2/cyclin A among all reported peptides of similar length.

Either histone (*24*) or ATP (*31*, *59*) alone has been demonstrated to bind to all forms of CDK2 except in the case of the [unP]CDK2 monomer, for which protein substrate binding has not been measured (*24*). Thus, the mechanism of substrate addition is predicted to be random. Direct measurement of the binding constants for histone H1 in the absence of ATP (*24*) indicates the corresponding K_d values to be significantly lower than those inferred from kinetic measurements carried out in saturating ATP (*31*). However, the disparate experimental conditions and approaches employed necessitate extreme caution in these interpretations.

The kinetic reaction pathway of [P]CDK2/cyclin A (Scheme 1) is similar whether histone peptide or protein is used as substrate, in terms of the kinetic parameters linked to both turnover and ATP binding (*31*). However, while the catalytic efficiency of histone protein phosphorylation is at least 5-fold greater (*31*), the most complete set of kinetic data has been obtained using the peptide as substrate. In saturating ATP, histone peptide binds the active site in rapid equilibrium fashion with $K_m \approx 8\ \mu M$; $K_d \approx 25\ \mu M$, and turns over with rate contants $35\ s^{-1}$ for phosphoryl transfer and $9\ s^{-1}$ for product release (*31*). The role of phosphorylation of CDK2/cyclin A at Thr^{160} is to substantially (44-fold) increase the affinity of peptide substrate binding (Table 3) (*47*). The enhanced substrate affinity may be correlated with movement of the activation loop such that the carbonyl oxygen of Val^{163} is rotated out of the P_{+1} substrate binding pocket, allowing access of the P_{+1} proline to the active site (*50*). In contrast, phosphorylation exerts no significant effect on the affinity for ATP (*31*). Thus, in both CDK2/cyclin A and ERK2, the effect of threonine phosphorylation (step 2, Figures 1 and 2) is to enhance substrate binding, with no effect on affinity for the nucleotide.

Phosphorylation also serves to enhance the rate of phosphoryl transfer to the peptide by 2650-fold (*47*) and to histone H1 by 1000-fold (Table 3) (*31*). These rate enhancements are larger than those corresponding to ERK2 (60-fold) (*53*). However, similar to ERK2, phosphorylation at threonine does not affect the rate of phosphoryl transfer to water in the ATPase reaction of CDK2/cycin A (Table 3) (*31*, *60*). Thus, in both enzymes, threonine phosphorylation serves to stabilize the binding and reactivity of the protein substrate exclusively—there are no effects on ATP.

In ERK2, all parameters linked to ATP are under the control of phosphorylation at Tyr^{185} (*53*). Similarly, in cdk2, there is modest increase in ATP affinity (*59*), and significant increase in ATPase phosphoryl transfer rate upon cyclin binding (Table 3) (*31*, *60*). Thus, while kinetic data are limiting on the role of cyclin, it appears that cyclin binding to CDK2 may serve a somewhat analogous role to Tyr^{185} phosphorylation in ERK2. Regardless, similarities in the kinetic activation mechanisms of ERK2 and CDK2 are particularly apparent with respect to the kinetic role of threonine phosphorylation (Figures 3 and 4). It should be noted that the respective roles of cyclin binding versus threonine phosphorylation in CDK2 are not as cleanly separable as those of tyrosine versus threonine phosphorylation in ERK2.

Of particular interest is the apparent role of cyclin in lowering the binding energy for histone protein. Crystallographic information reveals that substrates are unable to bind to monomeric CDK2 because the activation loop sterically hinders access of substrates to the active site (*22*). Cyclin binding results in dramatic movement of the activation loop (*23*), which, in the case of [P]CDK2, corresponds to a minimum 480-fold increased affinity for histone protein (*31*). Importantly, K_m^{H1} is enhanced by over 1000-fold, while the corresponding increase in k_{cat} is only 8.8-fold (step 4, Figure 2, Table 3) (*31*). This implies that catalytic inhibition in the absence of cyclin is due mainly to a competitive mechanism, providing kinetic proof that cyclin acts mainly to facilitate histone binding, as opposed to optimizing the structure of the active site.

CONCLUSIONS

Over the past several years, kinetic information has begun to accrue on the catalytic mechanisms of several protein kinases (*17*). While structure/function analysis is the traditional application of mechanistic work, it may be anticipated that kinetic analyses will play an increasingly broader role in systems biology on a whole. For example, mathematical modeling and computer simulation will undoubtedly gain prominence as a tool for cell function analysis on a global level. Already a lucid example is provided by the demonstration of *all-or-none signaling* in protein kinase cascades by mathematical simulation techniques (*61*−*64*). While it is anticipated that genomic analysis will allow all proteins in a given cellular process to be identified, cell function by computational analysis will necessarily depend on knowledge of experimentally determined kinetic parameters of all components involved. Since it cannot be assumed that biochemical reactions necessarily operate in the steady-state in cells, knowledge of the microscopic kinetic constants will be required.

We have reviewed here the basic kinetic mechanism for activation of the CDK2 and ERK2 kinases. While this is currently the most detailed information of its type, essentially only substrate binding and chemistry have been described. The role of conformational changes, the effect of mutations (both natural and engineered), and the characterization of physiological substrates are the most relevant areas for future investigation. Given the ubiquitous role of protein kinases in cellular homeostasis, their kinetic characterization will likely bring new insight into all aspects of cell function.

SUPPORTING INFORMATION AVAILABLE

Appendix of key methodology and references, including descriptions of solvent viscosometric techniques and data analysis. This material is available free of charge via the Internet at http://pubs.acs.org.

REFERENCES

1. Krebs, E. G. (1989) *JAMA 262*, 1815−8.
2. Krebs, E. G. (1998) *Annu. Rev. Biochem. 67*, xii−xxxii.
3. Hunter, T. (2000) *Cell 100*, 113−27.
4. Hanks, S. K., Quinn, A. M., and Hunter, T. (1988) *Science 241*, 42−52.
5. Hanks, S. K., and Hunter, T. (1995) *Faseb J. 9*, 576−96.
6. Soderling, T. R. (1990) *J. Biol. Chem. 265*, 1823−6.
7. Johnson, L. N., and Lewis, R. J. (2001) *Chem. Rev. 101*, 2209−42.
8. Johnson, L. N., Noble, M. E., and Owen, D. J. (1996) *Cell 85*, 149−58.
9. Harper, J. W., and Adams, P. D. (2001) *Chem. Rev. 101*, 2511−26.
10. Knighton, D. R., Zheng, J. H., Ten Eyck, L. F., Ashford, V. A., Xuong, N. H., Taylor, S. S., and Sowadski, J. M. (1991) *Science 253*, 407−14.
11. Knighton, D. R., Zheng, J. H., Ten Eyck, L. F., Xuong, N. H., Taylor, S. S., and Sowadski, J. M. (1991) *Science 253*, 414−20.
12. Smith, C. M., Radzio-Andzelm, E., Madhusudan, Akamine, P., and Taylor, S. S. (1999) *Prog. Biophys. Mol. Biol. 71*, 313−41.
13. Taylor, S. S., and Radzio-Andzelm, E. (1994) *Structure 2*, 345−55.
14. Gibbs, C. S., and Zoller, M. J. (1991) *J. Biol. Chem. 266*, 8923−31.
15. Carrera, A. C., Alexandrov, K., and Roberts, T. M. (1993) *Proc. Natl. Acad. Sci. U.S.A. 90*, 442−6.
16. Robinson, M. J., Harkins, P. C., Zhang, J., Baer, R., Haycock, J. W., Cobb, M. H., and Goldsmith, E. J. (1996) *Biochemistry 35*, 5641−6.
17. Adams, J. A. (2001) *Chem. Rev. 101*, 2271−90.
18. Chen, Z., Gibson, T. B., Robinson, F., Silvestro, L., Pearson, G., Xu, B., Wright, A., Vanderbilt, C., and Cobb, M. H. (2001) *Chem. Rev. 101*, 2449−76.
19. Canagarajah, B. J., Khokhlatchev, A., Cobb, M. H., and Goldsmith, E. J. (1997) *Cell 90*, 859−69.
20. Russo, A. A., Jeffrey, P. D., and Pavletich, N. P. (1996) *Nat. Struct. Biol. 3*, 696−700.
21. Zhang, F., Strand, A., Robbins, D., Cobb, M. H., and Goldsmith, E. J. (1994) *Nature 367*, 704−11.
22. De Bondt, H. L., Rosenblatt, J., Jancarik, J., Jones, H. D., Morgan, D. O., and Kim, S. H. (1993) *Nature 363*, 595−602.
23. Jeffrey, P. D., Russo, A. A., Polyak, K., Gibbs, E., Hurwitz, J., Massague, J., and Pavletich, N. P. (1995) *Nature 376*, 313−20.
24. Brown, N. R., Noble, M. E., Lawrie, A. M., Morris, M. C., Tunnah, P., Divita, G., Johnson, L. N., and Endicott, J. A. (1999) *J. Biol. Chem. 274*, 8746−56.
25. Meijer, L., Leclerc, S., and Leost, M. (1999) *Pharmacol. Ther. 82*, 279−84.
26. Sielecki, T. M., Boylan, J. F., Benfield, P. A., and Trainor, G. L. (2000) *J. Med. Chem. 43*, 1−18.
27. Lewis, T. S., Shapiro, P. S., and Ahn, N. G. (1998) *Adv. Cancer Res. 74*, 49−139.
28. Jones, S. M., and Kazlauskas, A. (2001) *Chem. Rev. 101*, 2413−23.
29. Prowse, C. N., Hagopian, J. C., Cobb, M. H., Ahn, N. G., and Lew, J. (2000) *Biochemistry 39*, 6258−66.
30. Waas, W. F., and Dalby, K. N. (2002) *J. Biol. Chem. 277*, 12532−40.
31. Stevenson, L. M., Deal, M. S., Hagopian, J. C., and Lew, J. (2002) *Biochemistry 41*, 8528−34.
32. Blacklow, S. C., Raines, R. T., Lim, W. A., Zamore, P. D., and Knowles, J. R. (1988) *Biochemistry 27*, 683−733.
33. Brouwer, A. C., and Kirsch, J. F. (1982) *Biochemistry 21*, 1302−7.
34. Adams, J. A., and Taylor, S. S. (1992) *Biochemistry 31*, 8516−22.
35. Robbins, D. J., and Cobb, M. H. (1992) *Mol. Biol. Cell 3*, 299−308.
36. Haystead, T. A., Dent, P., Wu, J., Haystead, C. M., and Sturgill, T. W. (1992) *FEBS Lett. 306*, 17−22.
37. Ferrell, J. E., Jr., and Bhatt, R. R. (1997) *J. Biol. Chem. 272*, 19008−16.
38. Burack, W. R., and Sturgill, T. W. (1997) *Biochemistry 36*, 5929−33.
39. Clark-Lewis, I., Sanghera, J. S., and Pelech, S. L. (1991) *J. Biol. Chem. 266*, 15180−4.
40. Gonzalez, F. A., Raden, D. L., and Davis, R. J. (1991) *J. Biol. Chem. 266*, 22159−63.
41. Songyang, Z., Lu, K. P., Kwon, Y. T., Tsai, L. H., Filhol, O., Cochet, C., Brickey, D. A., Soderling, T. R., Bartleson, C., Graves, D. J., DeMaggio, A. J., Hoekstra, M. F., Blenis, J., Hunter, T., and Cantley, L. C. (1996) *Mol. Cell Biol. 16*, 6486-93.
42. Weston, C. R., Lambright, D. G., and Davis, R. J. (2002) *Science 296*, 2345−7.
43. Grant, B. D., and Adams, J. A. (1996) *Biochemistry 35*, 2022−9.

44. Shaffer, J., Sun, G., and Adams, J. A. (2001) *Biochemistry 40*, 11149−55.
45. Stewart, R. C. (1997) *Biochemistry 36*, 2030−40.
46. Robbins, D. J., Zhen, E., Owaki, H., Vanderbilt, C. A., Ebert, D., Geppert, T. D., and Cobb, M. H. (1993) *J. Biol. Chem. 268*, 5097−106.
47. Hagopian, J. C., Kirtley, M. P., Stevenson, L. M., Gergis, R. M., Russo, A. A., Pavletich, N. P., Parsons, S. M., and Lew, J. (2001) *J. Biol. Chem. 276*, 275−80.
48. Madhusudan, Trafny, E. A., Xuong, N. H., Adams, J. A., Ten Eyck, L. F., Taylor, S. S., and Sowadski, J. M. (1994) *Protein Sci. 3*, 176−87.
49. Zheng, J., Knighton, D. R., ten Eyck, L. F., Karlsson, R., Xuong, N., Taylor, S. S., and Sowadski, J. M. (1993) *Biochemistry 32*, 2154−61.
50. Brown, N. R., Noble, M. E. M., Endicott, J. A., and Johnson, L. N. (1999) *Nat. Cell Biol. 1*, 438−443.
51. Lowe, E. D., Noble, M. E., Skamnaki, V. T., Oikonomakos, N. G., Owen, D. J., and Johnson, L. N. (1997) *EMBO J. 16*, 6646−58.
52. Prowse, C. N., and Lew, J. (2001) *J. Biol. Chem. 276*, 99−103.
53. Prowse, C. N., Deal, M. S., and Lew, J. (2001) *J. Biol. Chem. 276*, 40817−23.
54. Zhou, B., and Zhang, Z. Y. (2002) *J. Biol. Chem. 277*, 13889−99.
55. Solomon, M. J., and Kaldis, P. (1998) *Results Probl. Cell Differ. 22*, 79−109.
56. Connell-Crowley, L., Solomon, M. J., Wei, N., and Harper, J. W. (1993) *Mol. Biol. Cell 4*, 79−92.
57. Felix, M. A., Labbe, J. C., Doree, M., Hunt, T., and Karsenti, E. (1990) *Nature 346*, 379−82.
58. Beaudette, K. N., Lew, J., and Wang, J. H. (1993) *J. Biol. Chem. 268*, 20825−30.
59. Heitz, F., Morris, M. C., Fesquet, D., Cavadore, J. C., Doree, M., and Divita, G. (1997) *Biochemistry 36*, 4995−5003.
60. Holmes, J. K., and Solomon, M. J. (2001) *Eur. J. Biochem. 268*, 4647−52.
61. Ferrell, J. E., Jr. (1997) *Trends Biochem. Sci. 22*, 288−9.
62. Ferrell, J. E., Jr., and Machleder, E. M. (1998) *Science 280*, 895−8.
63. Ferrell, J. E., Jr. (1996) *Trends. Biochem. Sci. 21*, 460−6.
64. Huang, C. Y., and Ferrell, J. E., Jr. (1996) *Proc. Natl. Acad. Sci. U.S.A. 93*, 10078−83.

BI0269761